

# Cholesteric Mesophases Formed by the Modified Biological Macromolecule 3,6-*O*-(Butyl Carbamate)-*N*-phthaloyl Chitosan

Deeleep K. Rout, Shikha P. Barman, Satish K. Pulapura, and Richard A. Gross\*

Department of Chemistry, University of Massachusetts, Lowell, One University Avenue, Lowell, Massachusetts 01854

Received December 1, 1993; Revised Manuscript Received March 7, 1994\*

**ABSTRACT:** Cholesteric liquid crystalline phases were observed in dimethyl sulfoxide solutions of a new chitosan derivative. This chitosan derivative had a substitution pattern which approximates that of 3,6-*O*-(butyl carbamate)-*N*-phthaloyl chitosan (BuCaPhCh). UV-visible and circular dichroic (CD) spectroscopy carried out on BuCaPhCh revealed that the cholesteric pitch is in the visible wavelength ( $\lambda$ ) region and is left-handed for all investigated polymer weight fraction,  $x$ , values (0.50, 0.56, 0.60, and 0.70) and solution temperatures (25–88 °C). The apparent absorption maxima,  $\lambda_a$ , due to selective reflection of the cholesteric phases, showed a very strong variation as  $x$  was decreased to a value near the isotropic–anisotropic solution liquid crystal transition. The change in pitch as a function of temperature ( $dP/dT$ ) was negative for all of the polymer weight fractions investigated. It was determined that the pitch–temperature relationship was dissimilar in two different temperature regions: (I)  $\infty \geq [1 - T_c/T] \geq 1.25$  and (II)  $1.25 \geq [1 - T_c/T] \geq 0$ , where  $T_c$  is the clearing temperature. Use of the empirical relationship  $(1/\lambda_a) \sim (1 - T_c/T)^\nu$  showed that the exponent,  $\nu$ , within the normalized temperature region II, varies considerably (0.05–0.22) as a function of the  $x$  value, whereas, in the normalized temperature region I,  $\nu$  is almost independent of the  $x$  value. A comparison was carried out of the experimental pitch–temperature–concentration relationships determined herein relative to that expected on the basis of theoretical relationships proposed by Varichon, Ten Bosch, and Sixou (*Liq. Cryst.* 1991, 9, 701). It was found that there was very good agreement between theory and experiment for pitch–polymer concentration dependence. In contrast, the experimental pitch–temperature dependence showed poor agreement with that expected on the basis of theoretical predictions.

## Introduction

Cholesteric liquid crystal phases have been observed in various lyotropic solutions of synthetic and naturally derived macromolecules. Important examples of mesophases obtained from natural and biomimetic structures include polypeptides,<sup>1</sup> proteins,<sup>2</sup> poly(nucleic acids),<sup>3</sup> and polysaccharides.<sup>4</sup> Chiroptical measurements recorded by optical rotatory dispersion (ORD) and circular dichroism (CD) have been used to measure the pitch and helicoidal twist sense and twisting power of cholesteric phases. Much of the study of cholesteric mesophases has been directed toward poly( $\gamma$ -benzyl L-glutamate), PBLG,<sup>1</sup> cellulose derivatives,<sup>5</sup> and selected optically active polymers, such as polyisocyanates.<sup>6</sup> In most of these polymer liquid crystalline systems, with few exceptions,<sup>7</sup> the cholesteric pitch has a linear dependence with changes in the sample temperature.

Theoretical models have been proposed by a number of investigators to help predict the behavior of chiral nematic lyotropic mesophases.<sup>8</sup> A molecular statistical theory for cholesteric liquid crystals was proposed by Lin–Liu et al.,<sup>9</sup> in which chiral contributions were included in the intermolecular potential term. This theory, however, did not take into account the characteristics of the mesophase as a function of the solvent, and therefore, fails to explain the dramatic effects that the solvent may have on the pitch as well as on the handedness of the macroscopic helix. Osipov<sup>10</sup> constructed a theory that considered both steric and attractive interactions in the calculation for intermolecular potential. The effect of the dielectric nature of the solvent surrounding the rodlike or semirigid molecules was also taken into account. Osipov's theory provides a very good qualitative explanation for the pitch–temperature relationship for these rodlike polymers. More recently, Varichon et al.<sup>11</sup> extended Lin–Liu's molecular

statistical theory by considering the contribution of orientational entropy terms. In this theoretical model, pitch is considered as a ratio of symmetric to chiral asymmetric interactions. The concentration dependence of pitch can be given either by dilution of chiral interactions, leading to an increase of the pitch, by dilution of the symmetric nematic interactions, leading to a decrease of the pitch, or by considering the complex interactions resulting from these two contributions. This theory predicts a large diversity of behavior by changing the ratio of the asymmetric chiral and the symmetric nematic interaction parameters. Semiquantitative agreement was possible in a recent analysis<sup>12</sup> on the effect of the degree of polymerization and degree of acetylation for acetoxypolypropyl cellulose and ethyl cellulose, respectively.

Recently, lyotropic liquid crystalline phases of site-selectively modified chitosans have been reported by our laboratory.<sup>13</sup> These modified polymers also form interesting anisotropic gels that exhibit unique thermal characteristics.<sup>14</sup> In this report, results are presented and discussed on a new site-selectively modified chitosan which approximates the substitution pattern 3,6-*O*-(butyl carbamate)-*N*-phthaloyl chitosan (BuCaPhCh). It is shown that BuCaPhCh exhibits well ordered cholesteric phases in concentrated dimethyl sulfoxide (DMSO) solutions. This is the first report of a modified chitosan polymer that formed well ordered cholesteric mesophases with correspondingly large selective reflection bands in the visible wavelength region. CD and UV-vis spectroscopy were used to study the pitch–temperature–concentration relationships for this derivative. The experimental results obtained were then compared with those predicted using the theoretical model developed by Varichon, Ten Bosch, and Sixou.<sup>11</sup>

\* Abstract published in *Advance ACS Abstracts*, April 15, 1994.

## Experimental Section

**Polymer Synthesis.** PhCh<sup>13</sup> (1 g, 3.7 mmol) was dissolved in 10 mL of DMF. Butyl isocyanate (4 mL, 350 mmol) was added followed by triethylamine (0.1 mL, 7.3 mmol), and the reaction mixture was stirred for 24 h at 60 °C. The reaction mixture was then cooled to room temperature and the product isolated by precipitation into ether. The polymer was collected by filtration, and further purified by Soxhlet extraction with ether for 24 h.

**Polymer Structural Analysis.** Molecular weight averages were determined by gel permeation chromatography (GPC). GPC analysis of BuCaPhCh was carried out using two PL-gel GPC columns (300 mm × 7.7 mm, particle size 5 mm, pore size 10<sup>5</sup> and 10<sup>3</sup> Å) placed in series and with DMF containing 0.1% (wt/vol) LiBr as the eluent. Molecular weights were calculated relative to polystyrene standards with no further corrections. The molecular weight averages ( $M_w$  and  $M_w/M_n$ ) of the polymer were found to be 271 000 and 2.17, respectively. The degrees of *O*-butyl carbamate, *N*-phthaloyl, and *O*-phthaloyl substitution (starting chitosan was 93% deacetylated) were determined from elemental analysis and <sup>1</sup>N NMR spectral integration, as was previously described,<sup>13</sup> and are 1.52, 0.93, and 0.52, respectively.

**Sample Preparation.** Concentrations ( $x$ ) of 0.5, 0.56, 0.60, and 0.70 by weight percent of the polymer in dimethyl sulfoxide (DMSO) solutions were prepared separately in small glass vials and were tightly capped with Teflon tape so that the solvent did not evaporate. The solutions were heated to 100 °C in a thermostated oven for about 10–15 min to improve the sample homogeneity. The sample homogeneity can be directly visualized in the vial from the uniformity of the reflecting color. The sample was then sandwiched between two precleaned glass plates. The thickness of the cells were predetermined by using either 50- $\mu$ m Mylar spacers or 18- $\mu$ m-diameter glass beads. The sandwiched cells were sealed from all the sides by using an epoxy (Devcon or Torr seal).

**Instrumental Methods for Mesophase Characterization.** The selective reflection wavelength of the cholesteric mesophases formed results in an apparent CD band which was measured using a Jasco J-710 CD spectrometer. This CD spectrometer was also used to record the linear absorption spectra of the mesophases in the 200–700-nm region. The temperature of the sample cells was controlled by a programmable temperature controller (Neslab RTE 110) under a N<sub>2</sub> purge with a temperature accuracy of better than 0.1 deg. The apparent absorption maxima was determined from the linear absorption spectra when the degree of rotation exceeded a limiting value of 2°. Clearing transition temperatures ( $T_c$ ) for various samples were determined by differential scanning calorimetry (DSC) using a DuPont DSC 2910 with a 2000 Thermal analyzer. In addition, thermal transitions were confirmed by polarizing light microscopy (PLM). PLM was performed using a Leitz Ortholux II microscope (with ×320 magnification) equipped with a Mettler FP 50/52 hot stage.

The intermolecular spacing, used in the theoretical calculations presented herein, was determined from a wide-angle X-ray diffractogram, performed with a Phillips X-ray diffractometer using Cu K $\alpha$  radiation with power settings of 40 kV and 20 mA. The scattered X-rays were collected using a scintillation counter at a rate of 500 counts/s. The sample was solvent cast on a zero background substrate. The solvent was slowly evaporated so that the film formed a liquid crystals phase prior to complete solvent removal. This ensured that the film retained the liquid crystalline ordering and did not recrystallize.

## Results and Discussion

**Experimental Pitch Variation with Temperature and Polymer Concentration.** The sample cells were prepared immediately after the polymer solutions were made and homogenized (see Experimental Section). No aging time was given to the sample cells before performing experiments. The sample cells with  $x$  values of 0.56, 0.60, and 0.70 all showed visible reflecting colors. At the relatively lower sample polymer weight fraction of  $x = 0.50$  no visible reflecting color was observed. From PLM observations, the critical concentration ( $x_c$ ) was found to be 0.5.

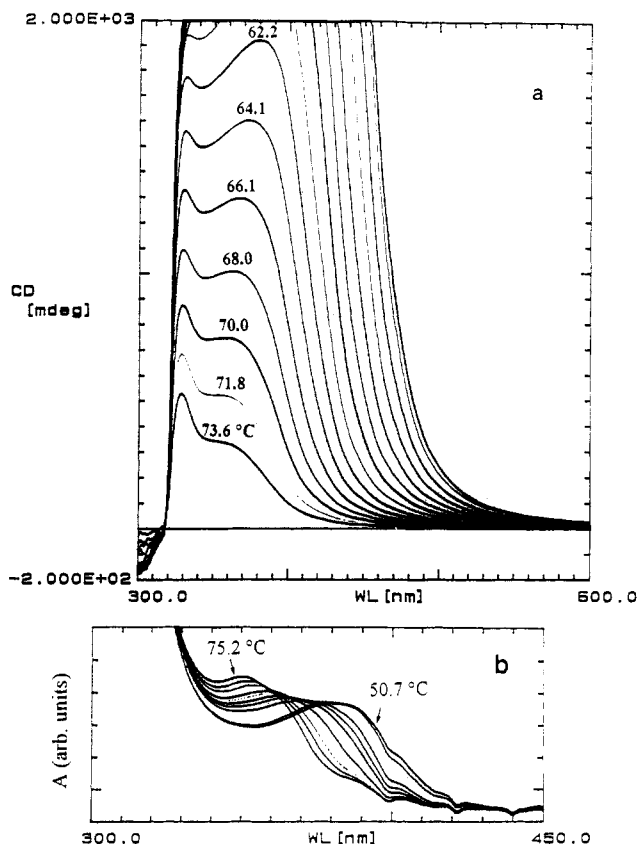


**Figure 1.** (a) Circular dichroic absorption spectra for BuCaPhCh-0.6-DMSO and (b) optical absorption spectra for BuCaPhCh-0.7-DMSO showing the shift of the band due to selective reflection with temperature.

The formation of liquid crystalline phases by BuCaPhCh-DMSO solutions was confirmed by PLM studies (see Experimental Section). Anisotropic solutions were investigated by UV-vis and CD spectroscopy. In addition to the UV absorption band at approximately 329 nm due to the phthaloyl chromophoric group,<sup>13,14</sup> a relatively weak UV band was observed at a higher wavelength, which is assigned as an apparent absorption with a peak at wavelength  $\lambda_a$  that is due to selective reflection from BuCaPhCh-DMSO cholesteric solutions (see Figure 1b). Furthermore, very strong, wide and positive CD bands exceeding 2° were observed at wavelengths corresponding to the above mentioned relatively weak apparent absorption band, which are also attributed to selective reflections of BuCaPhCh-DMSO cholesteric mesophases (see Figure 1a). The positive sign of the CD band, as per convention, indicates that the cholesteric phases have a left-handed helicoidal twist sense. Figure 1 also shows decreases in the  $\lambda_a$  as well as the intensity of the corresponding CD band as the temperature of the mesophase is increased.

Figure 2 shows the variation of  $\lambda_a$  ( $\lambda_a = nP$  where  $n$  is the refractive index and  $P$  is the cholesteric pitch) with the polymer weight fraction ( $x$ ) of the solution at four different temperatures. An interesting feature observed is the large increase in  $\lambda_a$  from  $x = 0.50$  to 0.56 and subsequent decrease with increasing  $x$ . Therefore, a very strong variation in  $\lambda_a$  values was observed near  $x_c$ . Such a large variation of pitch near  $x_c$  has not been observed before for other lyotropic, cholesteric mesophases. The  $x = 0.5$  sample did not show a very strong apparent CD band intensity when compared with samples with relatively higher  $x$  values. For example, the respective magnitudes of the CD absorption at  $\lambda_a$  and at a temperature of ( $T_c - 20$ ) °C for samples with  $x = 0.5$  and 0.6 are 37 and 1922 mdeg, respectively. The sample thicknesses in both the

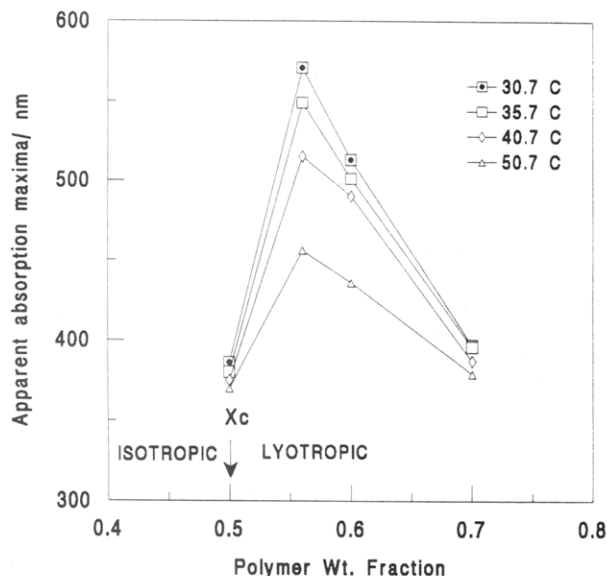


**Figure 2.** Variation of apparent absorption maxima  $\lambda_a$  with increasing polymer concentration in the solution at four different temperatures showing a strong variation near the isotropic-anisotropic transition.

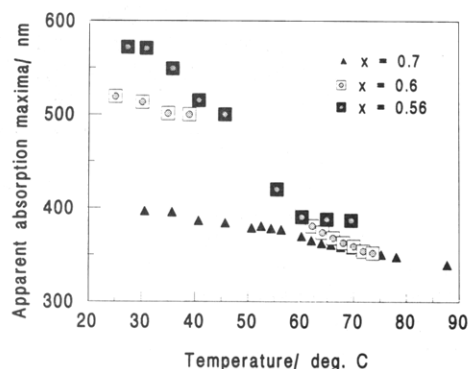


**Figure 3.** Variation of the apparent absorption maxima  $\lambda_a$  with temperature ( $d\lambda_a/dT$ ) for samples having different polymer concentrations ( $x = 0.56, 0.6, 0.7$ ). For these samples,  $d\lambda_a/dT$  was negative. For most of the cellulose derivatives previously investigated  $d\lambda_a/dT$  was found to be positive except for some derivatives, such as ethyl cellulose dissolved in acetic acid,<sup>15</sup> chloroform, aqueous phenol, *m*-cresol,<sup>16</sup> acetyl ethyl cellulose solutions with chlorinated and phenolic solvents,<sup>16</sup> cellulose acetate,<sup>17</sup> cellulose triacetate,<sup>18</sup> and methyl cellulose.<sup>16</sup> Additionally, the pitch-temperature variation was larger for the BuCaPhCh-*x*-DMSO of relatively lower concentration ( $x = 0.56$ ; see Figure 3).

samples were almost identical ( $\sim 18 \mu\text{m}$ ). Therefore, it is concluded that the transition to a liquid crystalline phase had taken place at  $x = 0.5$  but a well ordered planar cholesteric organization had not as yet formed.

Figure 3 shows the variation in  $\lambda_a$  as a function of temperature ( $d\lambda_a/dT$ ) for samples having different polymer concentrations ( $x = 0.56, 0.6, 0.7$ ). For these samples,  $d\lambda_a/dT$  was negative. For most of the cellulose derivatives previously investigated  $d\lambda_a/dT$  was found to be positive except for some derivatives, such as ethyl cellulose dissolved in acetic acid,<sup>15</sup> chloroform, aqueous phenol, *m*-cresol,<sup>16</sup> acetyl ethyl cellulose solutions with chlorinated and phenolic solvents,<sup>16</sup> cellulose acetate,<sup>17</sup> cellulose triacetate,<sup>18</sup> and methyl cellulose.<sup>16</sup> Additionally, the pitch-temperature variation was larger for the BuCaPhCh-*x*-DMSO of relatively lower concentration ( $x = 0.56$ ; see Figure 3).

The cholesteric-isotropic transition temperature was reported to increase with increasing polymer concentration in the solution for polypeptide systems.<sup>1</sup> In the present system, a linear increase in the clearing transition,  $T_c$ , was observed for solutions with  $x$  values increasing from 0.5 to 0.7 (see Figure 4). This information on the variation of  $T_c$  as a function of  $x$  was then used to investigate the empirical power law relationship between the inverse pitch ( $1/\lambda_a$ ) and the normalized temperature  $[(1/\lambda_a) \sim (1 - T_c/T)]$  for solutions with different polymer concentrations.

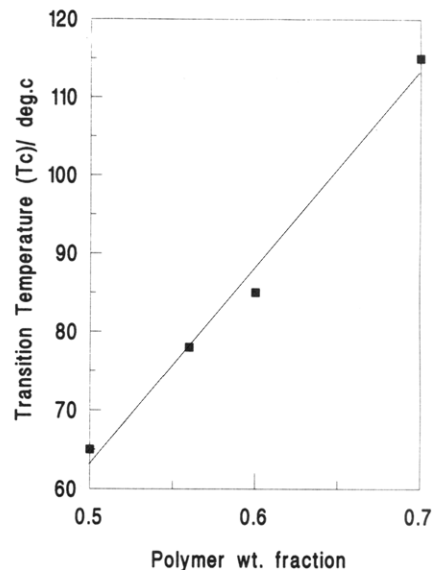


**Figure 4.** Linear dependence of transition temperature  $T_c$  with polymer concentration.

The motivations for this analysis were to (i) obtain a generalized picture of  $(1/\lambda_a)$  versus temperature behavior in a manner so as to compensate for differences in  $T_c$  for lyotropic solutions of different polymer concentrations and (ii) observe how the physically measurable parameter  $\lambda_a$  which is directly associated with the organization of the lyotropic cholesteric liquid crystal varies in the mesophase region as well as near the phase transition. This analysis also allows us to not include the proportionality constant for  $(1/\lambda_a) \sim (1 - T_c/T)^\nu$  which is known to have a complex dependence upon many parameters including the nature of the solvent, polymer molecular weight, and molecular geometry. Thus, it is expected that the exponent  $\nu$ , which is the slope in a double logarithmic plot of  $(1/\lambda_a)$  versus  $(1 - T_c/T)$ , might be the same irrespective of the sample concentration and temperature range investigated. It is interesting to note that there are two distinctly different slopes for each of the four curves constructed for BuCaPhCh-*x*-DMSO solutions where  $x$  is 0.50, 0.56, 0.6, and 0.7 (see Figure 5). Therefore, it can be concluded that the pitch-temperature relationships for these lyotropic solutions were dissimilar in two different temperature regions; the low temperature region (I) where  $\infty \geq |1 - T_c/T| \geq 1.25$  and the relatively higher temperature region (II) which approaches  $T_c$  where  $1.25 \geq |1 - T_c/T| \geq 0$ . In region I,  $\nu$  values for the three solutions are nearly the same. The  $\nu$  values derived from the empirical relationship  $(1/\lambda_a) \sim (1 - T_c/T)^\nu$  for these mesophases in temperature region I were found to be approximately 0.05. In contrast, in temperature region II, the slopes change with mesophase concentration. The exponents in region II where  $T_c - T \leq 65^\circ\text{C}$  for solutions with  $x = 0.56, 0.6, 0.7$  were found to be 0.22, 0.07, and 0.06, respectively. Therefore, the behavior of  $\nu$  in the two respective temperature regions was found to be drastically different for BuCaPhCh-DMSO cholesteric mesophases.

**Comparisons between Theory and Experimental Results.** The interaction potential between two rodlike molecules at positions  $\mathbf{r}_1$  and  $\mathbf{r}_2$  and with respective orientations  $\Omega_1$  and  $\Omega_2$  is given by eq 1,<sup>11</sup> where the first

$$V(\mathbf{r}_1, \mathbf{r}_2, \Omega_1, \Omega_2) = V_N(\mathbf{r}_{12}, \Omega_1, \Omega_2) + (\Omega_1 \Omega_2 \cdot \mathbf{r}_{12}) V_x(\mathbf{r}_{12}, \Omega_1, \Omega_2) \quad (1)$$

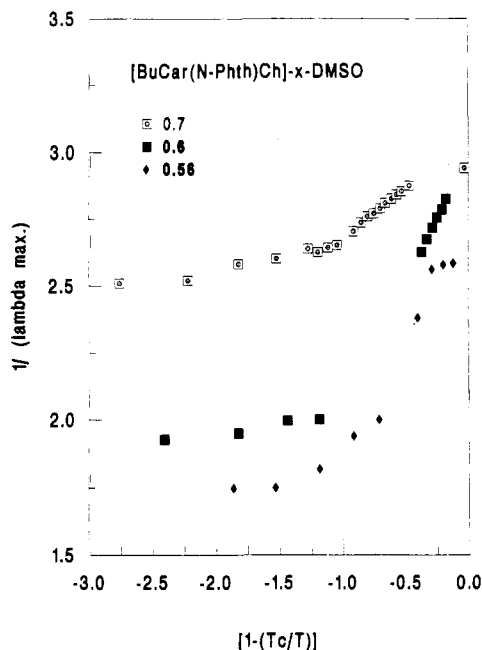


**Figure 5.** Variation of  $(1/\lambda_a)$  with normalized temperature  $(1 - T_c/T)$  showing two different regimes, in which pitch varies differently with temperature.

and second right hand side terms of the equation are the orientation dependent nematic orientation potential and the chiral interaction potential, respectively. The Helmholtz free energy for a chiral nematic liquid crystal system contains nematic, chiral contributions in addition to isotropic contributions. Thus, taking into account the contribution of orientational entropy (nematic field) as well as the chiral mean field, Varichon, Ten Bosch, and Sixou<sup>11</sup> developed a theory, where the pitch,  $P$ , can be expressed as

$$Q = 2\pi d/P = [n_0 + \{(\bar{x}n_1 + \bar{x}^2n_2)/n\}]/[(\lambda_2/\gamma_2) + \{(\bar{x}d_1 + \bar{x}^2d_2)/n\}] \quad (2)$$

with the symbols defined as follows:

$$n_0 = m_1 + m_2 S^2(T)$$

$$n_1 = 4m_1/5$$

$$n_2 = -\{8\sigma_2(T)/35\}\{m_1 + m_2 S(T)\}$$

$$d_1 = 2[2/5\{(\lambda_2/\gamma_2) + 3m_1^2\} + \{(2/3)m_2^2 S(T)^2\}]$$

$$d_2 = -2\sigma_2(T)[(4/35)\{(\lambda_2/\gamma_2) + 6m_1^2\} + \{(48/35)S(T)m_1m_2\} + \{(80/231)m_2^2 S(T)^2\}]$$

$$n = 2 + \{(\bar{x}^2/5)\sigma_2^2(T)\}$$

$$\bar{x} = x(L\gamma_2/kT_c)(T_c/T) \quad S(T) = \{\sigma_4(T)/\sigma_2(T)\}$$

$$m_1 = \{(\mu_1/3) - (\mu_3/7)\}(1/\gamma_2) \quad m_2 = (10/21)(\mu_3/\gamma_2)$$

$$\gamma_2 = \int V_2(\eta) d\eta \quad \lambda_2 = -\int (\xi_2^2 V_2(\eta) d\eta)$$

$$\mu_m = \int (\xi_2^2/\eta) V_m(\eta) d\eta \quad \eta = r/d \quad \xi = z/d$$

The  $z$ -axis is defined as the optical axis. The important parameters are as follows: reduced concentration,  $\bar{x}$ ;  $S(T)$

which is the ratio of the second order,  $\sigma_2(T)$ , and fourth order,  $\sigma_4(T)$ , order parameters;  $m_1$ , which is the ratio of chiral interactions of first ( $\mu_1$ ) and third ( $\mu_3$ ) order in the expansion of the intermolecular potential  $V_m$  for spherical harmonics; the average nematic field,  $\gamma_2$ ; and the ratio  $m_2$  of the chiral interactions of the third order and the nematic field. The position vector,  $\mathbf{r}$ , and the  $z$ -axis are normalized with respect to the intermolecular distance  $d$  and are defined as  $\xi$  and  $\eta$ , respectively. Similarly, the temperatures are also normalized with respect to the anisotropic-isotropic transition,  $T_c$ .  $\lambda_l$ ,  $l = 2, 4$ , are the nematic (symmetric) interaction parameters of the second and fourth order in the expansion of the intermolecular potential  $V_l$ .

Our objectives were (i) to determine the numerical values of  $(\mu_3/\gamma_2)$  and  $(\mu_1/\gamma_2)$  from eq 1 by utilizing data from the experimental  $\lambda_a \sim T$  relationship and then (ii) to compare the experimental and theoretical pitch-polymer concentration as well as pitch-mesophase temperature trends for an identical set of  $(\mu_3/\gamma_2)$  and  $(\mu_1/\gamma_2)$  values. To do this, eq 1 was first simplified, which yields a coupled quadratic equation with roots  $m_1$  and  $m_2$ . From the values of  $m_1$  and  $m_2$ ,  $(\mu_3/\gamma_2)$  and  $(\mu_1/\gamma_2)$  were calculated.

Thus, experimental values of pitch ( $\lambda_a$ ), polymer concentration, and temperature were taken from the determined  $\lambda_a \sim T$  relationship for  $x = 0.7$  (Figure 5). For the mesophase solution with  $x = 0.7$ ,  $T_c$  was found to be 115 °C and the  $\lambda_a$  values at 30.6, 50.7, 60.1, and 87.7 °C were 397, 379, 370, and 343 nm, respectively. The temperatures 30.6, 50.7, and 60.1, 87.7 °C fall into the temperature regions I and II, respectively (see Figure 5). The intermolecular distance ( $d$ ) was determined from an X-ray diffractogram. A relatively sharp and a broad peak were observed in the polymer film cast from a liquid crystalline solution, which correspond to  $d$  spacings of 13.8 and 4.3 Å, respectively. The sharp peak arises due to the intermolecular spacing, and thus for our calculation purpose the intermolecular spacing  $d$  value was taken as 13.8 Å. Similar values for intermolecular spacings were also found in liquid crystalline cellulose derivatives.<sup>16</sup> The order parameters  $S(T)$  and  $\sigma_2(T)$  were determined from the theoretical fit of the following equations<sup>11</sup>

$$S(T) = S(T_c) + 0.42 \exp\{-7.31/(T_c - T)\} \quad (3)$$

$$\sigma_2(T) = 0.28(T_c - T)^{0.26}\{(1.15)^{1/(T_c - T)}\} \quad (4)$$

In this evaluation, the order parameter at the transition temperature  $S(T_c)$  was assumed to be zero. The conditions of validity for eq 3, specifically when  $T < (T_c - 0.65)$  is satisfied in the present case.  $\sigma_2$  and  $S$  values for temperatures 30.6, 50.7, 60.1, and 87.7 °C are 0.88, 0.83, 0.79, 0.66 and 0.38, 0.37, 0.36, 0.31, respectively. The mean field value for  $(kT_c/L\gamma_2)$ , taken from the Maier-Saupe relation<sup>19</sup> is -0.22. Also, the value used for  $\lambda_2/\gamma_2$  herein is the same as that in the ref 11 and is equal to -2.

Using the numerical values for the relevant parameters as mentioned in the preceding paragraphs, the coupled quadratic equation (1) with roots  $m_1$  and  $m_2$  was solved and the values less than 1 were retained.<sup>20</sup> Thus, we determined the values for  $(\mu_3/\gamma_2)$  and  $(\mu_1/\gamma_2)$  for the two different temperature regions I and II mentioned above. The values for  $(\mu_3/\gamma_2)$  in regions I and II are -0.005 and -0.004, respectively. Similarly, the values for  $(\mu_1/\gamma_2)$  in regions I and II are -0.012 and -0.011, respectively. These values thus obtained from the experimental results herein are comparable to a set of values  $(\mu_3/\gamma_2) = -0.004$  and  $(\mu_1/\gamma_2) = -0.04$  used for theoretical predictions.<sup>11</sup> The

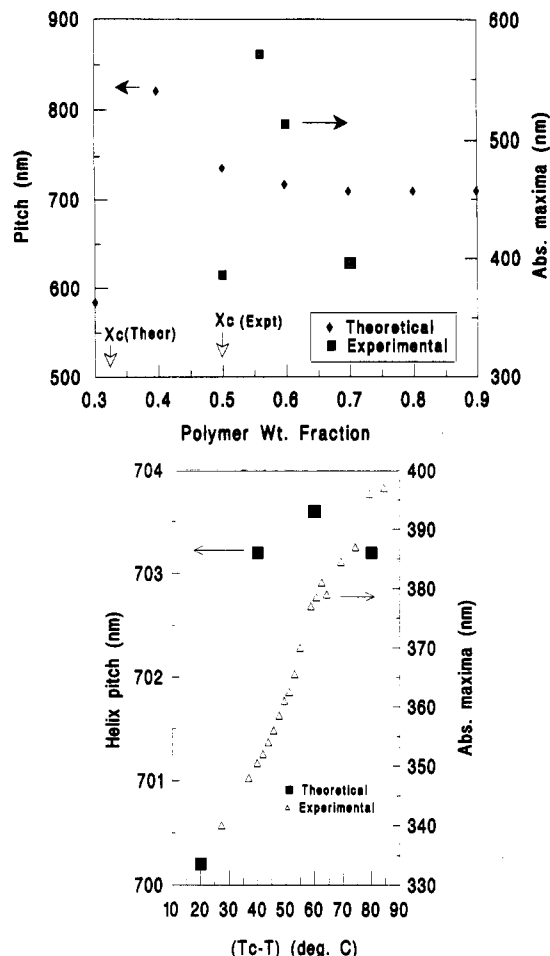


**Figure 6.** Plots of theoretical (replotted from ref 11, Figure 1a,b, respectively) and experimental (a, top)  $P$  (or  $\lambda_a$ )  $\sim x$  and (b, bottom)  $P$  (or  $\lambda_a$ )  $\sim T$  behavior.

experimental  $\lambda_a$  versus  $x$  and  $\lambda_a$  versus  $T$  relationships were then compared with the theoretical trends shown in Figure 1a,b in ref 11. Figure 6a shows the theoretical (replotted from ref 11, Figure 1a)  $P$  and experimental  $\lambda_a$  versus  $x$  plots. It is evident from Figure 6a that there is a very strong variation in both the theoretical pitch and experimental  $\lambda_a$  values near the isotropic-liquid crystal transition ( $x_c$ ). This transition to the anisotropic liquid crystal phase in BuCaPhCh-DMSO took place at  $x_c = 0.5$ . The corresponding  $x_c$  in the theoretical curve is  $\sim 0.3$ .

A comparison between theoretical  $P$  and experimental (BuCaPhCh-0.7-DMSO)  $\lambda_a$  versus  $T_c - T$  (Figure 6b) revealed that both  $P$  and  $\lambda_a$  increase with decreasing temperature (increasing  $T_c - T$ ). However, above  $(T_c - T) = 60$  °C, theoretical  $P$  decreases in contrast to the experimental  $\lambda_a$ , which continues to increase up to  $(T_c - T) = 84$  °C (the maximum observed value). Thus, the important features of our analysis are as follows:

(i) There is very good agreement between theory and the experimental results obtained herein for the variation of theoretical  $P$  and experimental  $\lambda_a$  with changes in  $x$ . A strong variation in the pitch near the isotropic-anisotropic transition is expected theoretically and was indeed observed. Furthermore, both experiment and theory showed that for  $x$  values well above  $x_c$ , the pitch decreased with increasing concentration of the polymer in solution.

(ii) The agreement between the theoretical prediction and experimental results for the variation of theoretical  $P$  and experimental  $\lambda_a$  as a function of temperature was found to be poor. As evident in Figure 6b, both experimental and theoretical helix pitch increase with decreasing temperature (increasing  $T_c - T$ ) up to  $(T_c - T) \approx 60$  °C,

but at  $(T_c - T) > 60$  °C the theoretical pitch decreases in contrast to the experimental pitch (or  $\lambda_a$ ). Also, the magnitude of theoretical pitch variation over the total temperature interval is only 4 nm. In contrast, the magnitude of variation in experimental pitch over the identical temperature interval is  $\sim 30$  nm (assuming  $n = 1.5$ ). This indicates that there is a significant variation of helix pitch with temperature in lyotropic cholesteric mesophases such as was observed in the BuCaPhCh-DMSO system, but the present theoretical analysis does not provide for such a strong variation.

In the present calculation, both  $\mu_1$  and  $\mu_3$  were found to be positive. This indicates that repulsive interactions dominate over polar attractive forces for the formation of lyotropic BuCaPhCh-DMSO mesophases. Therefore, the introduction of butyl carbamate and phthaloyl side chain substituents onto chitosan appears to limit chain-chain interactions. However, the magnitude of  $\mu_1/\gamma_2$  ( $= -0.01$ ) in the present calculation is smaller than the value  $-0.04$  considered in previous theoretical work.<sup>12</sup> At present, it is not understood by us how the absolute magnitude of  $\mu_1/\gamma_2$  affects the relationships  $P$  ( $\lambda_a$ ) versus  $x$  or  $P$  ( $\lambda_a$ ) versus  $T$ . We have also calculated the  $\mu_1/\gamma_2$  value for other BuCaPhCh- $x$ -DMSO samples with  $x = 0.6$  and  $0.56$ . No significant deviation in the value of  $\mu_1/\gamma_2$  as a function of  $x$  was found. In addition, the effect of the magnitude of  $|R|$  ( $= (\mu_1/\mu_3)$ ) on  $P$ - $T$  behavior is not clear. The theoretically predicted  $P$ - $T$  relationship is not consistent throughout the mesophase region, especially near the clearing transition. The authors attributed this to the use of values of the order parameters  $S$  and  $\sigma_2$  which were greater than would be expected. The concentration and temperature gradient of pitch were also shown to be considerably affected by the order of expansion in  $x$  in the theoretical treatment, which is undesirable considering the fact that the higher order terms are considerably smaller than the first order terms and should act as perturbative correction factors. This would account for the poor agreement between the theoretically predicted pitch and experimental  $\lambda_a$  results obtained herein as a function of temperature.

## Summary of Conclusions

The synthesis of BuCaPhCh was successfully carried out. It was shown that BuCaPhCh exhibits well ordered cholesteric phases in concentrated dimethyl sulfoxide (DMSO) solutions. This is to our knowledge the first report of a lyotropic, cholesteric liquid crystal formed by the modification of chitosan that has a helix pitch comparable to visible wavelengths. The cholesteric pitch in the lyotropic liquid crystalline phase of BuCaPhCh in DMSO shows a strong variation at polymer concentrations near the isotropic-anisotropic transition. The pitch varies nonlinearly with temperature, contrary to previously reported work on lyotropic cholesteric mesophases exhibited by either polypeptides or polysaccharides. In addition, the behavior of the pitch as a function of temperature was distinctly different in temperature regions I and II which may result from subtle changes in polymer concentration as a function of the mesophase temperature.

The predictability of  $P$  or  $\lambda_a$  as a function of  $T$  and  $x$  using the model developed by Varichon, Ten Bosch, and Sixou for lyotropic or thermotropic cholesteric mesophases, which takes into account the orientational entropic effects in addition to the helicoidal twist (chiral mean field terms), was evaluated using our experimental results on pitch-concentration and pitch-temperature relationships for BuCaPhCh-DMSO mesophases. The agreement between

theoretically predicted and experimental results was very good for changes in pitch resulting from alterations in the mesophase polymer concentration. In contrast, poor agreement was found between results obtained experimentally and those predicted by the theoretical model for pitch change as a function of the mesophase temperature.

**Acknowledgment.** Financial support of this work by the National Science Foundation, Division of Materials Research, under a Presidential Young Investigator award (R.A.G., Grant DMR-9057238), is gratefully acknowledged. We thank Prof. Mark Green of the Polytechnic University (Brooklyn, NY) for valuable comments on the manuscript. We are also thankful for the technical assistance on X-ray studies provided by Mike Downey of the Center for Advanced Materials at the University of Massachusetts Lowell.

## References and Notes

- (1) Uematsu, I.; Uematsu, Y. *Adv. Polym. Sci.* **1984**, *59*, 37.
- (2) Bernal, J. D.; Fankuchen, I. *J. Gen. Physiol.* **1941**, *25*, 111; Perutz, M. F.; Liquory, A. M.; Eirich, S. *Nature* **1951**, *167*, 929.
- (3) Yevdokimov, Yu. M.; Skuridin, S. G.; Salyanov, V. L. *Liq. Cryst.* **1988**, *3*, 1443. Livolant, F. *Physica A* **1991**, *176*, 117. Rill, R. L.; Strzelecka, T. E.; Davidson, M. W.; Van Winkle, D. H. *Physica A* **1991**, *176*, 87.
- (4) Triethyl- and trimethylamylose in chloroform (Zugenmeier, P.; Voitsel, M. *Macromol. Chem. Commun.* **1984**, *5*, 245). Xanthan (Maret, G.; Milas, M.; Rinando, M. *Polym. Bull.* **1981**, *4*, 291. Bouligand, Y.; Livolant, F. *J. Phys. (Paris)* **1984**, *45*, 1899). Schizophyllan and scleroglucan (Van, K.; Asakawa, T.; Teramoto, A. *Polym. J.* **1984**, *16*, 1661. Chitin microfibrils (Revol, J. F.; Bradford, H.; Giasson, J.; Marchessault, R. H.; Gray, D. G. *Int. J. Biol. Macromol.* **1992**, *14*, 170. Cellulosics (Werbosy, R. S.; Gray, D. G. *Mol. Cryst. Liq. Cryst. Lett.* **1976**, *34*, 97). Sixou, P.; Ten Bosch, A. In *Cellulose Structure, Modification and Hydrolysis*; Young, R. A., Rowell, R. M., Eds.; Wiley-Interscience: New York, 1986; p 205.
- (5) Harkness, B. R.; Gray, D. G. *Macromolecules* **1990**, *23*, 1452. Aden, M. A.; Bianchi, E.; Cifferi, A.; Conio, G.; Teladi, A. *Macromolecules* **1984**, *17*, 2010. Guo, J.; Gray, D. G. *Macromolecules* **1989**, *22*, 2082 and references therein.
- (6) Green, M. M.; Christiani, B.; Andreolla, C.; Sato, T.; Nagamura, Y.; Wagner, J.; Okamoto, Y.; Teramoto, A. *Polym. Prepr. (Am. Chem. Soc., Div. Polym. Chem.)* **1991**, *32* (10), 453. Sato, T.; Sato, Y.; Uemura, Y.; Teramoto, A.; Nagamura, Y.; Wagner, J.; Weng, D.; Okamoto, Y.; Hatada, K.; Green, M. M. *Macromolecules* **1993**, *26*/17, 4551.
- (7) Guo, J.-X. Ph.D. Thesis, McGill University, 1992.
- (8) Kimura, H.; Hosino, M.; Nakano, H. *J. Phys. Soc. Jpn.* **1982**, *51*/5, 1584.
- (9) Lin-Liu, Y. R.; Shih, Y. M.; Woo, C. W. *Phys. Rev. A* **1977**, *15*, 2550.
- (10) Osipov, M. A. *Chem. Phys.* **1985**, *96*, 259. Osipov, M. A. *Nuovo Cimento Soc., Ital. Fis.* **1988**, *10D*, 1249.
- (11) Varichon, L.; Ten Bosch, A.; Sixou, P. *Liq. Cryst.* **1991**, *9*, 701.
- (12) Varichon, L.; Ten Bosch, A. *Macromolecules* **1992**, *25*, 3812.
- (13) Rout, D. K.; Pulapura, S. K.; Gross, R. A. *Macromolecules* **1993**, *26*, 5999.
- (14) Rout, D. K.; Pulapura, S. K.; Gross, R. A. *Macromolecules* **1993**, *26*, 6007.
- (15) Vogt, U.; Zugenmaier, P. *Ber. Bunsen-Ges. Phys. Chem.* **1985**, *89*, 1217.
- (16) Guo, J.-X.; Gray, D. G. *Macromolecules* **1989**, *22*, 2082; 2086.
- (17) Lematre, J.; Dayan, S.; Sixou, P. *Mol. Cryst. Liq. Cryst.* **1982**, *84*, 267.
- (18) Meeten, G. H.; Navard, P. *Polymer* **1982**, *23*, 1727.
- (19) Stephen, M. J.; Straley, J. P. *Rev. Mod. Phys.* **1974**, *46*, 617.
- (20) ( $\mu_1/\gamma_2$ ) and ( $\mu_3/\gamma_2$ ) with values less than 1 are only considered. It was found in ref 12 that only values less than 1 give the most reasonable temperature dependence.